Journal of Electromyography and Kinesiology 39 (2018) 149–155

Contents lists available at ScienceDirect

Journal of Electromyography and Kinesiology

journal homepage: www.elsevier.com/locate/jelekin

Surface electromyography can quantify temporal and spatial patterns of activation of intrinsic human foot muscles

E. Ferrari[a,*], G. Cooper[b], N.D. Reeves[a], E.F. Hodson-Tole[a]

[a] School of Healthcare Science, Manchester Metropolitan University, Manchester, UK
[b] University of Manchester, Manchester, UK

ARTICLE INFO

Keywords:
Surface EMG
Intrinsic foot muscles
Topographical mapping
Sample entropy

ABSTRACT

Intrinsic foot muscles (IFM) are a crucial component within the human foot. Investigating their functioning can help understand healthy and pathological behaviour of foot and ankle, fundamental for everyday activities. Recording muscle activation from IFM has been attempted with invasive techniques, mainly investigating single muscles. Here we present a novel methodology, to investigate the feasibility of recording physiological surface EMG (sEMG) non-invasively and quantify patterns of activation across the whole plantar region of the foot. sEMG were recorded with a 13 × 5 array from the sole of the foot (n = 25) during two-foot stance, two-foot tiptoe and anterior/posterior sways. Physiological features of sEMG were analysed. During anterior/posterior epochs within the sway task, sEMG patterns were analysed in terms of signal amplitude (intensity) and structure (Sample Entropy) distribution, by evaluating the centre of gravity (CoG) of each topographical map. Results suggest signals are physiological and not affected by loading. Both amplitude and sample entropy CoG coordinates were grouped in one region and overlapped, suggesting that the region with highest amplitude corresponds with the most predictable signal. Therefore, both spatial and temporal features of IFM activation may be recorded non-invasively, providing opportunity for more detailed investigation of IFM function in healthy and patient populations.

1. Introduction

The human foot is critical for a wide range of activities of daily living. Foot pathologies and deformities, can have a major impact on a person's quality of life, with significant associated costs for healthcare providers. Issues associated with foot health can be structural (e.g. hallux valgus, pes cavus) and/or functional (e.g. hallux limitus and hallux rigidus) and can be associated with a range of chronic diseases such as diabetes mellitus where peripheral neuropathy and foot ulcerations are common. Understanding the features of good foot health and characteristics that underpin appropriate function is therefore important in a range of health-related fields.

The anatomy of the foot is complex, with different segments interacting to provide a flexible structure and facilitate motion (Kelly et al., 2014; Bates et al., 2013; McKeon et al., 2015). There are four layers of intrinsic muscles arranged within the narrow compartment of the plantar region (McKeon et al., 2015) (Fig. 1). Their anatomical positioning provides challenges to quantifying features of anatomy and activation during weight bearing tasks. Intrinsic foot muscle properties have been investigated using a number of techniques including electromyography (EMG), to investigate muscle activation patterns. The majority of EMG studies use invasive intramuscular techniques, focusing on a single or a small selection of muscles in the foot region (Kelly et al., 2012, 2014). Whilst providing useful insight, these approaches cannot be applied to problematic populations (e.g. diabetes patients) and cannot quantify activity across the whole foot region and so, interactions between or within regions of the intrinsic foot muscles cannot be probed, although such information is required for wider aspects of foot function to be evaluated in healthy and pathological populations.

One method of quantifying activation across a larger region is to use multi-channel electrode arrays. The use of a large number of electrodes within a grid, allows the processing of myoelectric signals as topographical maps quantifying both spatial and temporal features of signals (Rojas-Martínez et al., 2013; Holtermann et al., 2008). Due to heterogeneity either in the distribution of activated motor units or the strategy of recruitment, the spatial distribution of myoelectric intensity measures can change over time (Farina et al., 2008). Therefore, analysis of maps of sEMG intensities could quantify patterns of activation within and between muscles in a confined anatomical space. Such techniques

* Corresponding author.
E-mail address: elisabetta.ferrari@stu.mmu.ac.uk (E. Ferrari).

https://doi.org/10.1016/j.jelekin.2018.02.009
Received 15 February 2018; Accepted 20 February 2018

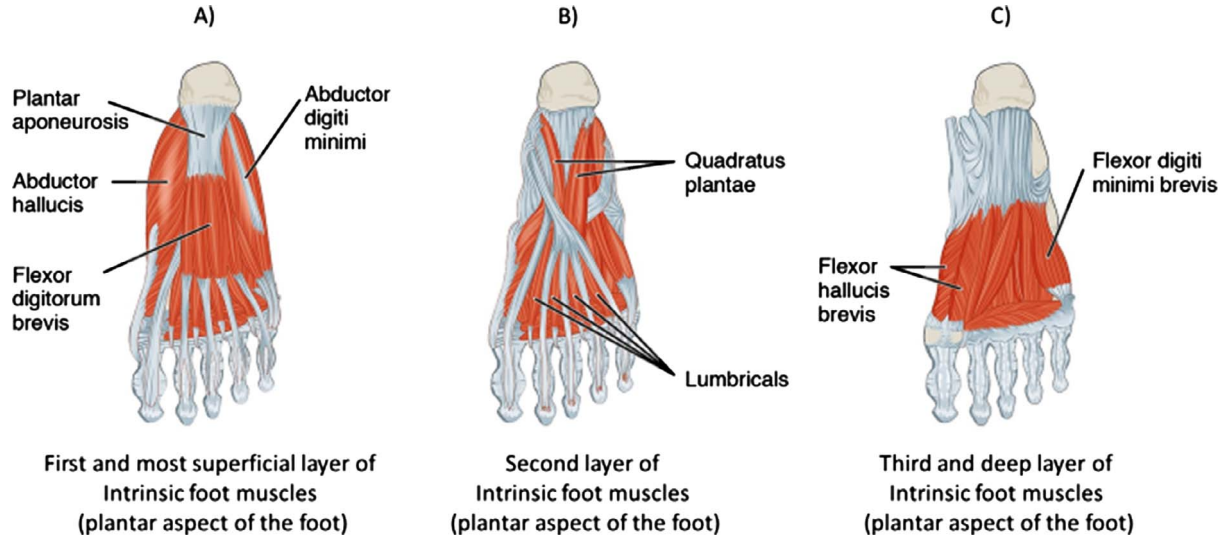

Fig. 1. Representation of the first three layers of the intrinsic foot muscles. Panel (A) shows the most superficial muscles, Panel (B) shows the second layer and Panel (C) the third and deep layer. The image has been amended from OpenStax (2016) down loaded from: https://commons.wikimedia.org/wiki/File:1124_Intrinsic_Muscles_of_the_Foot.jpg.

have been applied to different regions of the body (Falla and Farina, 2008; Gallina and Botter, 2013; Tucker et al., 2009; Rodriguez-Falces et al., 2013). However, to date, there have been no attempts to investigate the features of intrinsic foot muscle activation through the plantar surface of the foot using multi-channel systems.

In addition to traditional measures of sEMG intensities, changes in the complexity of motor patterns have recently been related to changes in motor strategies and muscle firing patterns (Rathleff et al., 2011), quantified with the use of Sample Entropy (SampEn). SampEn is defined as the negative natural logarithm of the conditional probability that two sequences are similar to m points and remain similar at the next point, $m + 1$ (Richman and Moorman, 2000). Greater SampEn values indicate a more complex signal structure and lower predictability of the time series (Richman and Moorman, 2000). To our knowledge, such analysis approaches have not previously been applied to explore variations in signal characteristics across a muscle region nor to study characteristics of intrinsic foot muscle activity.

Commercially available electrode arrays are flat and flexible and can be applied to the contours of the plantar region of the foot. However, these arrays have not been used previously on the foot region, as one concern is that loading due to body weight could influence signal characteristics. As such, signal amplitude changes could represent the movement of electrodes toward/away from the intrinsic foot muscles, rather than the physiological neuromuscular activation. Therefore, the aim of this work was to use a commercially available multi-channel array in a novel application to intrinsic foot muscles and to investigate whether it is possible to non-invasively quantify physiologically relevant temporal and spatial activation patterns from the plantar foot surface to provide new information about the human foot in health and disease.

2. Methods

2.1. Participants

Twenty-five healthy participants (twenty-two males and three females, age: 41 ± 15 years, weight: 73 ± 16 kg, height: 1.7 ± 0.1 m) voluntarily took part in the study having provided informed, written consent to do so. All procedures were approved by the local ethics committee in the Faculty of Science and Engineering at Manchester Metropolitan University. Exclusion criteria for participants included foot pain or lower limb pain during the last six months.

2.2. Data acquisition

Monopolar sEMGs were collected from the intrinsic foot muscles with a high-density grid of 64 channels (ELSCH model, OT Bioelettronica, Turin, Italy), consisting of 13 rows and five columns, with one missing electrode (2 mm diameter, 8 mm inter-electrode distance in both directions). Prior to attaching the grid of electrodes, the skin of the plantar region of the right foot was lightly abraded with abrasive paste and cleaned to remove any debris. To determine the array location, the adipose pads at the heel and toes were palpated and the grid positioned between these regions with the columns along the longitudinal axis of the foot (Fig. 2). A conductive cream (Spesmedica, Italy) was inserted into each cavity of the grid to assure proper electrode skin interface. The reference electrode was positioned around the right ankle.

Three-dimensional motion data were recorded using a 9-camera motion-capture system (Vicon Motion Systems, Oxford, UK) positioned around a force plate (Advanced Mechanical Technology, Inc., AMTI, Watertown, Massachusetts, USA) with an accuracy of ± 0.4 mm, which was covered with a 50 mm thick Styrofoam layer to reduce electrical noise from the ground. Fifty-four reflective markers were position on anatomical landmarks to track whole body movement. The Plug-in Gait marker set was utilised for anatomical landmarks on the shoulder to knee epicondyle and, from the tibial tuberosity to the foot, a modified Heidelberg foot marker set (Simon et al., 2006) was applied, with an additional marker on the shank to reduce problems associated with marker occlusion.

Each participant stood in the test area and was instructed to perform three motor tasks: (i) two-foot quiet standing (self-selected stance width); (ii) deliberate anterior/posterior sways (following a metronome beating at 2 Hz) and (iii) two foot continuous standing on tiptoe. These conditions were selected as they provided a range of quasi-static and motion-based conditions, and also provided one condition where there was no contact between the ground and the electrode grid meaning EMGs would be free from external loading. Each trial lasted 30 s. Synchronisation between force plate, motion capture data and EMG signals was achieved with the use of an external trigger.

2.3. Data analysis

Recorded sEMGs were visually inspected and channels showing noise due to poor skin-electrode interface contact or line interference were reconstructed based on the interpolation of the signals from

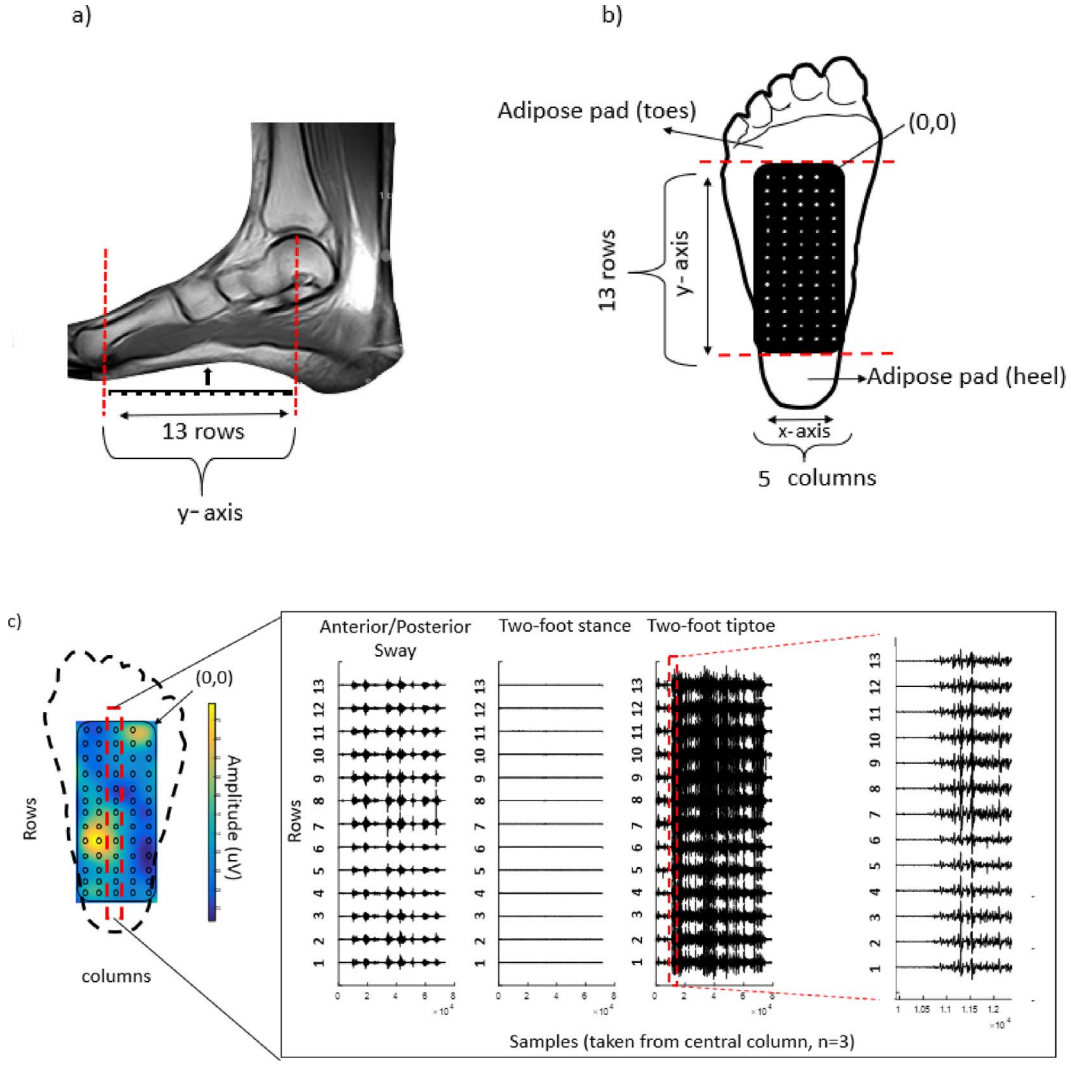

Fig. 2. Position of the 64 channel grid on the plantar region of the foot. (a) An MR image from one participant and the representation of the sEMG grid, positioned between the adipose tissue of the metatarsal heads and the heel pad; (b) the whole grid on the sole of the foot, with one missing electrode at the top left corner; (c) a representative map of monopolar EMG total intensity values distribution across the plantar region of the foot and a representative column from the grid showing clean EMG for each condition. It also shows a zoomed portion of the most active task (tiptoe), showing the signal window when the participant moved from standing quietly to tiptoeing.

neighbouring channels (Gallina and Botter, 2013). Wavelet analysis was used to process EMG signals following the protocol provided by (von Tscharner, 2000), where a filter bank of k wavelets was selected to represent a band-pass filter for the signal, with parameters set to ensure that the original signal intensities could be approximately reconstructed from the sum of the k-wavelet-transformed signals. In the present study, a filter bank of 11 ($0 \leq k \leq 10$) wavelets was used to decompose the myoelectric signals from each selected trial into their intensities. To remove low frequency artefacts, the signal from the first wavelet (10.16–33.20 Hz frequency band) was discarded so the total intensity at any given time was calculated as the sum of the intensities of the selected ($1 \leq k \leq 10$) wavelets (Hodson-Tole et al., 2012).

2.3.1. Investigation of physiological signal content

The first analysis step focused on identifying whether signals recorded were the result of physiological muscle activation and to what extent they were influenced by body weight pressure or potential movements of the array across the foot. Therefore, mean frequency and total intensity of myoelectric signals were calculated and compared to standard values presented in literature (Basmajian and De Luca, 1985) to determine how closely these features resembled previously reported physiological values.

As peaks saturating the signal amplitude might suggest non-physiological signal content, for example related to skin-electrode movement, the EMG amplitude was calculated. From the wavelet transformed signal, the total intensity is used as a measure of EMG intensity over time and the sum of total intensity approximates the description of power (von Tscharner, 2000). Half of the power can be seen as practically equal to the square of the root mean square (RMS) values, therefore the square root of half the power is equivalent to measures of amplitude such as RMS (von Tscharner, 2000; Wakeling et al., 2002). The mean frequency f_m (Wakeling et al., 2002; Hodson-Tole and Wakeling, 2007) of the intensity spectrum for each sample point is calculated from (Eq. (1):

$$fm = \frac{\sum_k f_c(k) i_k}{\sum_k i_{j,k}}, \tag{1}$$

where f_c is the central frequency of each wavelet and i is the intensity at each time point, j, and wavelet, k. Mean frequency was calculated for the entire length of each trial. Physiological signals in surface EMGs present the majority of frequency components between a range usually spanning 20–400 Hz (De Luca et al., 2010). If the signals collected showed frequency and amplitude components in the ranges reported in the literature, it can be suggested they are the result of

neuromuscular drive.

Secondly, whether EMG signal amplitudes were affected by changes in the position of the centre of pressure under the foot was investigated using trials from the anterior/posterior sway task. For this analysis, the centre of gravity (CoG_I) within the electrode grid was calculated, based on the spatial distribution of the EMG total intensity, and x and y co-ordinate of the maximum activation was extracted (Farina et al., 2008). If the signal amplitudes are affected by foot loading, we expect CoG_I to follow the same pattern of displacement as the biomechanical force plate derived centre of pressure (CoP), i.e. forward movement of the CoP should strongly correlate with forward movement of the EMG based CoG_I. If this relationship is not found, we posit that the sEMGs collected can be expected to be primarily representative of muscle activation and not predominantly the result of pressure on the electrode grid.

The force plate based CoP was calculated with Visual 3D (C-motion. Inc, Germantown, MD) and, when required, a bi-directional low-pass Butterworth filter was applied (6 Hz cut-off) before events corresponding to anterior and posterior sways were identified from the CoP path. The corresponding filtered wavelet-transformed myoelectric signals were down sampled to the same frequency at which force plate data were sampled (1000 Hz) and three events were identified in each signal: (i) start of anterior sway; (ii) end of anterior sway/start of posterior sway; (iii) end of posterior sway. The data points corresponding to these events were selected from the CoP trace, following manual inspection of signals. Respectively peaks and valleys of the CoP were selected, by visualising the transition of each participant during the task (e.g from anterior to posterior sway). For each epoch, the 64 channels intensity map was segmented to extract the region with the highest amplitude values using Otsu's algorithm (Chen et al., 2010). This approach allows segmentation without relying on potentially subjective thresholding, by minimising the weighted within-class variance and maximising the between class variance of the image (grid) intensity values. The CoG_I electrode grid co-ordinates in the medial/lateral (G_x) and anterior/posterior (G_y) direction were calculated for the segmented channels representing the highest activation. Once the sEMG CoG_I and force plate based CoP were extracted, the correlation between the two was calculated for the anterior and posterior sway epochs.

2.3.2. Quantifying sEMG complexity and amplitude during different movement tasks

In addition to identifying the physiological content of collected sEMG signals, we sought to investigate whether differences in movement patterns were associated with any changes in the sEMG amplitudes and complexity. Review of the biomechanical data revealed participants had completed the anterior/posterior sway trials using a variety of different strategies (i.e. swaying about the ankle joint vs around the hip joint). This variation in movement 'strategy' was therefore exploited to investigate the effects on features of recorded sEMG signals.

Firstly, to identify the movement strategy employed for each anterior and posterior sway event the ankle, knee and hip joint angles were calculated for each sway epoch. As the marker set used to track foot motion was a multi-segment model, it was also possible to calculate the angle between the rear-foot and the forefoot, corresponding to the angle from the medial longitudinal arch. A bi-directional low-pass Butterworth filter (6 Hz cut-off) was applied to marker tracks before angle calculation, when required, to remove high frequency noise due to skin-marker contact. For each epoch, the correlation between each joint angle and the CoP was evaluated and the joint with the largest correlation co-efficient was identified as the dominant joint for that movement.

The mean sEMG intensity distribution map was calculated for each anterior/posterior sway event. The CoG_I of each map was calculated by segmenting the regions showing activation higher than 80% of the maximum with Otsu's segmentation method (Chen et al., 2010). The x (medial/lateral) and y (anterior/posterior) coordinates of the CoG_I were respectively normalised to the width and length of the foot for each participant (foot width measured as the distance between the first and the fifth distal metatarsal; foot length from the hallux to the calcaneus).

SampEn values were calculated for sEMG data from the same anterior/posterior sway epochs. SampEn requires the selection of a tolerance value (r), and a length of segment (m), that corresponds to the number of data points checked, with:

$$\mathrm{SampEn}(m, r, N) = -\ln\frac{A^m(r)}{B^m(r)}, \tag{2}$$

where N is the length of the data set, r is the tolerance defined as the proportion of the standard deviation of the time series, A represents the count of matches for $m + 1$ and B the count of matches for m. Similar to previous reports (Zhang and Zhou, 2012), $r = 0.2$ and $m = 2$ were empirically chosen for this study.

For each epoch, the total intensity from the wavelet transformed myoelectric signal from each electrode channel was filtered with a high-pass filter (2nd order Butterworth filter, cut-off 10 Hz), to remove the slower temporal signal components, leaving components relating to oscillations in the envelope profile (Enders et al., 2015), before SampEn (Eq. (2) was calculated using an open-source software package (Goldberger et al., 2000). SampEn values were normalised to the SampEn value resulting from analysis of a randomly selected channel in the grid, where the data points were randomly shuffled prior to SampEn calculation. As a random sequence of data, the result should provide the highest value of SampEn meaning all normalised values would be ≤ 1. This analysis provided a map of 64 SampEn values, corresponding to the grid of electrodes, with one map produced per anterior/posterior sway epoch. These maps were segmented using the same Otsu segmentation applied to the amplitude data. Here a third layer of segmentation was introduced, resulting in a three layer map. The values between the first layer (greatest SampEn) and third layer (lowest SampEn) were discarded, so that CoG_{SE} was calculated for the lowest and highest SampEn, respectively. As with the amplitude data, the x (medial/lateral) and y (anterior/posterior) coordinate of CoG_{SE}, were respectively normalised to the width and length of the foot for each participant. Finally, to enable comparison of activation patterns between selected movement patterns, four categories were defined by the joint identified as dominate for the associated sway epoch. Each category corresponded to a specific joint and these are: ankle (ANK), knee (KN), hip (HIP) and medial arch (MA). Correlation values were evaluated between the angle of each joint and both amplitude and SampEn CoG values for each epoch. Epochs were then assigned to the relevant joint category based on the highest association found.

3. Results

3.1. Physiological signal content

The mean frequency and intensity values for each movement task are shown in Fig. 3 and were typical of physiological ranges reported in the literature (Basmajian and De Luca, 1985; Merletti and Parker, 2004). Intensity values were also in the range of those reported in previous studies (Kelly et al., 2012), recorded with intramuscular EMG during tasks of similar effort. Correlation between sEMG CoG_I and kinematics CoP showed no correlation during the anterior/posterior sway task ($r^2 = 0.067 \pm 0.060$, maximum: 0.127, p-values: 0.74 ± 0.26), indicating no relationship between motion and shift in the myoelectric CoG_I.

3.2. Relationship between sway movement and sEMG patterns

When comparing correlation coefficients between the CoP and each

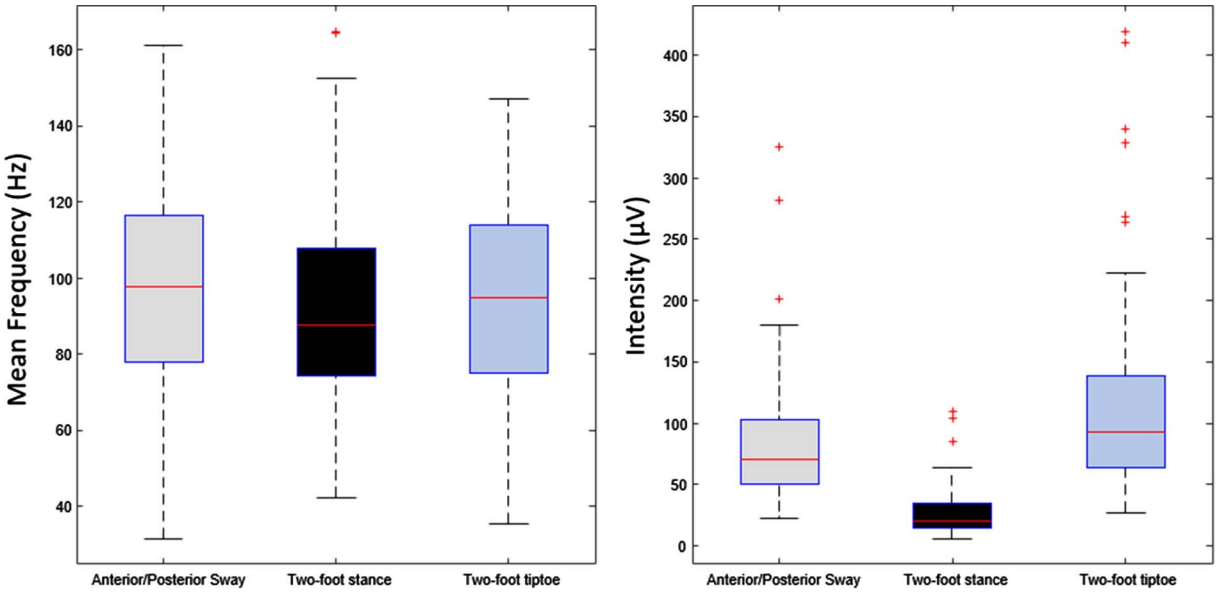

Fig. 3. Box and whisker charts for mean frequency (Left) and total intensity (Right) for the three tasks: (i) anterior/posterior sway (95.76 ± 33.17 Hz, 83.41 ± 52.75 μV, grey boxplot), (ii) two-foot stance (91.62 ± 27.32 Hz, 27.20 ± 20.27 μV, black boxplot), (iii) two-foot tiptoe (94.17 ± 29.32 Hz, 115.73 ± 79.24 μV, lightblue boxplot). The central mark indicates the median, and the bottom and top edges of the box indicate the 25th and 75th percentiles, respectively. The whiskers extend to the most extreme data points not considered outliers, and the outliers are plotted individually using the '+' symbol. (For interpretation of the references to colour in this figure legend, the reader is referred to the web version of this article.)

Table 1
Mean ± S.D. r^2 values from association between joint angle and CoP trace, used to define the dominant joint in each sway epoch. *n* indicates the number of epochs assigned to each joint.

		Medial Arch (MA)	Ankle (ANK)	Knee (KN)	Hip (HIP)
Anterior sways	r^2	0.896 ± 0.09 n = 104	0.855 ± 0.151 n = 42	0.891 ± 0.119 n = 52	0.80.0092 ± 0.035 n = 47
	p-values	0.00005 ± 0.00002	0.0013 ± 0.0051	0.0105 ± 0.442	0.0092 ± 0.104
Posterior sways	r^2	0.895 ± 0.113 n = 105	0.891 ± 0.114 n = 35	0.909 ± 0.09 n = 55	0.909 ± 0.0852 n = 52
	p-values	0.00001 ± 0.00005	0.00007 ± 0.00025	0.0047 ± 0.0194	0.0022 ± 0.0084

segment angles for each epoch during one trial, the highest correlation co-efficient commonly differed between each epoch within the same task. Across the group of 25 participants, the majority used three different dominant joints during the entire trial (one for each epoch). Table 1 shows the number of epochs (*n*) that each segment showed the highest correlation coefficient with the force plate CoP and the mean and standard deviation r^2 value and p-values for each group. The correlation was strong ($r^2 > 0.6$) for each of the four segments, but the joint most frequently identified as having the strongest correlation with CoP was the medial arch, whereas the least frequently identified joint was the ankle for both sway phases.

Fig. 4 shows mean and standard deviation for x and y coordinate of the location of the highest EMG activation and most structured signals for both anterior and posterior sways. Regardless of the dominant joint segment, both pair of coordinates were located within a relatively similar region. The region with the highest activation corresponded to the region where the signal is most structured and least random. CoG_I and CoG_{SE} are both in a region between the 15–37% of foot width and between the 14–32% of foot length, this region corresponds to the cluster of electrodes on the third column and seventh row of the grid, located towards the medial aspect of the foot.

4. Discussion

This study investigated whether it was possible to collect realistically physiological sEMG from intrinsic foot muscles using a multi-channel electrode array attached to the plantar surface of the foot. Features of the recorded signals (Fig. 3) suggest that they are representative of physiological muscle activation and are not adversely influenced by pressure on the electrode grid. The EMG total intensity increasing with task effort is in line with previous reports (using intramuscular data) where RMS values from quiet standing on two legs were lower than for standing on one leg (Kelly et al., 2012). The frequency values are within the physiological range (Merletti and Parker, 2004) with the highest mean frequency occurring during the anterior/posterior task. A key concern of using electrode arrays on the plantar foot surface was that signal characteristics would be significantly affected by changes in the point of pressure application under the foot. The results however clearly show no association ($r^2 = 0.067$) between CoG and CoP. In addition, the highest intensity values are for the two-foot tiptoe task, the only task where no interaction with the ground occurs, strongly indicating that the EMG signals recorded may be considered indicators of intrinsic foot muscle activation for the tasks assessed here.

During the anterior/posterior sway task participants were challenged to repeatedly and regularly change their posture. Kinematic and kinetic analysis showed that, within the same trial, the same participant commonly displayed different kinematics. Typically, the strongest association occurred between CoP and medial arch angle change (Table 1). In previous studies, the action of the medial arch has been suggested to be important for maintaining posture when performing a balancing task (Kelly et al., 2012). This could relate to the function of the intrinsic muscles as toe-flexors and, therefore, the high correlation between the sway movement and the medial arch here may reflect active gripping of the ground with the toes or passive extension/flexion of the joint with the changing centre-of-mass vector direction.

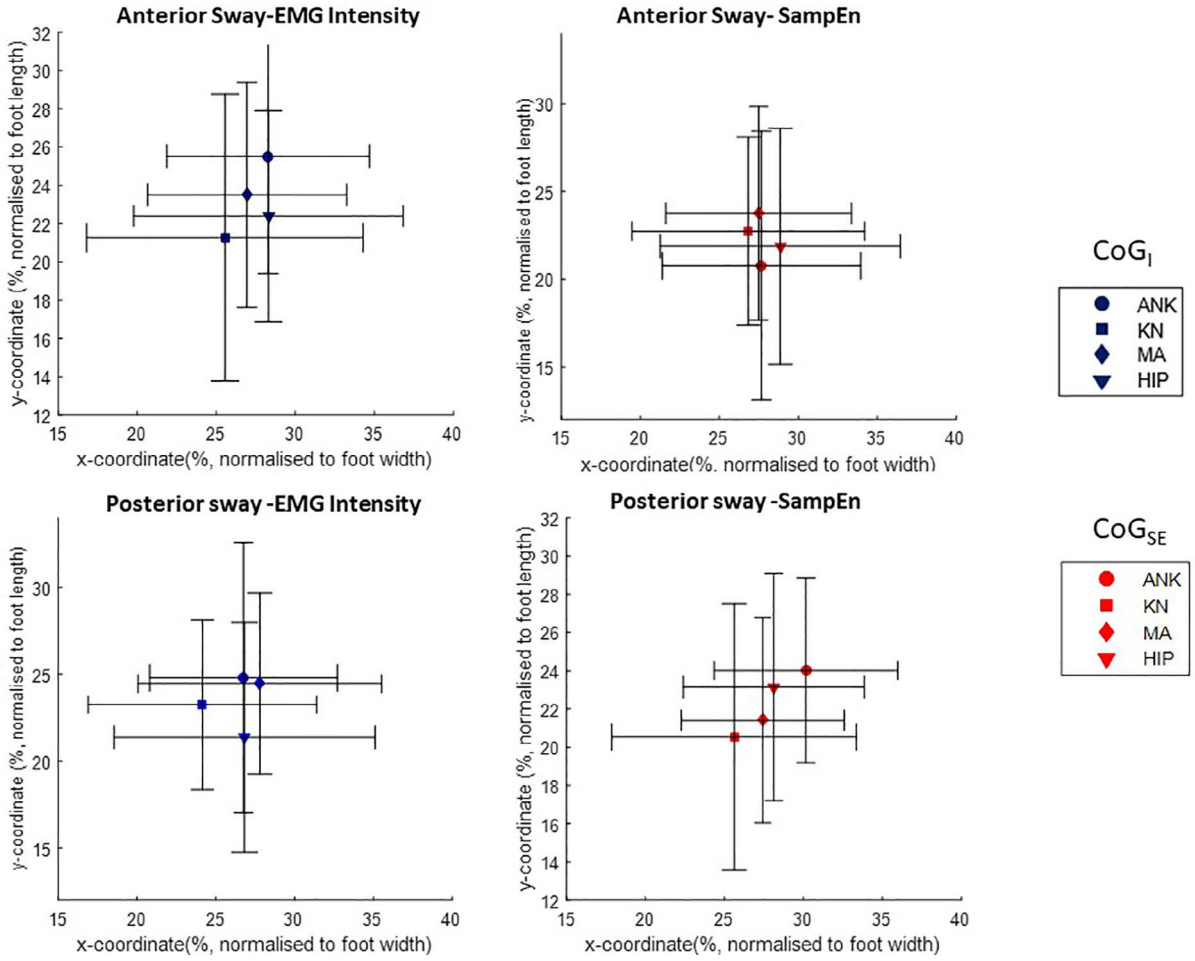

Fig. 4. Mean and standard deviation for CoG_I and CoG_{SE} co-ordinates. Data are split to show values for each dominant joint category: Medial arch (diamond); ankle (circle); knee (square) and hip (triangle).

During the anterior and posterior sways the mean position of CoG for both amplitude and SampEn did not show large differences in position, suggesting that the phase of movement nor the dominant joint had an effect on the regionalised pattern of activation in the intrinsic foot muscles. Both parameters are however grouped in one region, so the region with the highest activation and greatest signal structure coincided. The location is related to the region associated with the *Flexor Digitorum brevis* muscle, which is part of the most superficial layer of intrinsic foot muscles (Fig. 1). Future work should consider how other, deeper, muscles (e.g. *Quadratus plantae*) might contribute to such tasks, for example by exploiting the potential to extract depth information from surface arrays (Urbatek and Smagt, 2016). The clustered nature of the data presented here would be interesting to compare against data from clinical populations to explore whether variations might be indicative of different pathologies. For example: diabetes patients are at high risk of foot ulcer development, however changes in muscle activation have not been previously evaluated as a contributing risk factor; while aging affects stability and foot muscle weakness is one factor contributing to falls (Mickle et al, 2009). Studying and/or monitoring patterns of intrinsic foot muscle activation could therefore be beneficial for understanding neuromuscular contributions to foot stability and changes due to interventions such as exercise training (McKeon et al, 2015).

Although mean values for the position of highest activation and most structured signals did not differ significantly with movement pattern, differences were seen within individual participants, an example of which is shown in Fig. 5. Here the highest activation occurred during the hip and the lowest for the medial arch dominant movement. This may suggest that when flexing around the hip joint the intrinsic foot muscles actively facilitated the movement, while if the medial arch is more strongly associated with the changes in CoP, the foot is a more passive structure and extrinsic muscles may play a larger role in the task. Here, larger differences in the location of the intensity and SampEn based CoGs also occur when EMG intensity is lower (e.g. when medial arch is dominant). In the group data these differences are lost due to individual variation. Such variability might be related to the position of the grid on the foot with regard participant foot size; reflect differences in foot and intrinsic muscle morphology or differences in neuromuscular activation strategies. Placing the array in different positions (e.g. more under to toe pad or heel pad depending on foot size) could affect the results presented here and requires consideration if the arrays were to be applied in different orientations or regions of the foot; however the placement described here was chosen as it maximises the number of channels in the array overlaying the bulk of muscle tissue in the foot.

In conclusion, this study investigated the behaviour of intrinsic foot muscles using a surface multi-channel approach, which opens opportunity to collect data from participants where the insertion of a needle is not feasible, and enables exploration of temporal and spatial features of intrinsic foot muscle activation. It is therefore possible to non-invasively explore wider aspects of intrinsic foot muscle function to help inform understanding of foot muscle properties and function in health and disease. Future work should focus on different motion tasks, effects of pathology and the relationship between intrinsic and extrinsic foot muscles.

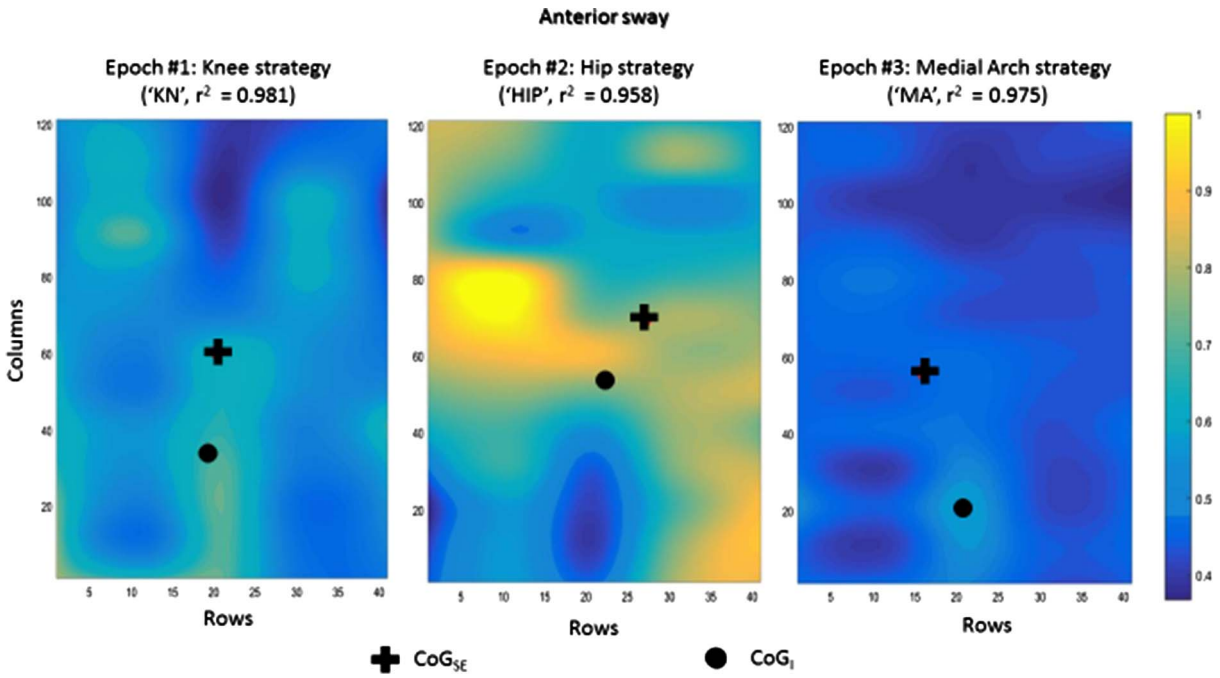

Fig. 5. Normalised topographical maps from one participant during anterior sways. A different dominant joint has been used by the participant for each event and differences in the activation patterns across the grid are evident.

Conflict of interest

The authors have no conflict of interest

Financial disclosure

We certify that no party having a direct interest in the results of the research supporting this article has or will confer a benefit on us or on any organization with which we are associated.

References

Basmajian, J.V., De Luca, C.J., 1985. Muscles alive: their functions revealed by electromyography.

Bates, K.T., Collins, D., Savage, R., McClymont, J., Webster, E., Pataky, T.C., Aout, K., Sellers, W.I., Bennett, M.R., Crompton, R.H., 2013. The evolution of compliance in the human lateral mid-foot. In: Proceedings of the Royal Society of London B: Biological Sciences, 280(1769).

Chen, Y., Chen, D.-R., Li, Y., Chen, L., 2010. In: 2nd International Asia Conference on Informatics in Control, Automation and Robotics: Otsu's Thresholding Method based on Gray Level-gradient Two-dimensional Histogram, vol. 3, pp. 282–285.

De Luca, C., Gilmore, D., Kuznetsov, M., Serge, H.R., 2010. Filtering the surface EMG signal: movement artifact and baseline noise contamination. J. Biomech. 43, 1573–1579.

Enders, H., Von Tscharner, V., Fau-Nigg, B.M., Nigg, B.M., 2015. Neuromuscular strategies during cycling at different muscular demands. Med. Sci. Sports Exerc. 47 (7), 1450–1459.

Falla, D., Farina, D., 2008. Non-uniform adaptation of motor unit discharge rates during sustained static contraction of the upper trapezius muscle. Exp. Brain Res. 191 (3), 363–370.

Farina, D., Leclerc, F., Arendt-Nielsen, L., Buttelli, O., Madeleine, P., 2008. The change in spatial distribution of upper trapezius muscle activity is correlated to contraction duration. J. Electromyogr. Kinesiol. 18 (1), 16–25.

Gallina, A., Botter, A., 2013. Spatial localization of electromyographic amplitude distributions associated to the activation of dorsal forearm muscles. Front. Physiol. 4, 367.

Goldberger, A.L., Amaral, L.A., Glass, L., Hausdorff, J.M., Ivanov, P.C., Mark, R.G., Mietus, J.E., Moody, G.B., Peng, C.K., Stanley, H.E., 2000. PhysioBank, PhysioToolkit, and PhysioNet: components of a new research resource for complex physiologic signals. Circulation 101 (23), 215–220.

Hodson-Tole, E.F., Wakeling, J.M., 2007. Variations in motor unit recruitment patterns occur within and between muscles in the running rat (*Rattus norvegicus*). J. Exp. Biol. 210, 2333–2345.

Hodson-Tole, E.F., Pantall, A., Maas, H., Farrell, B., Gregor, R.J., Prilutsky, B.I., 2012. Task-dependent activity of motor unit populations in feline ankle extensor muscles. J. Exp. Biol. 215 (21), 3711–3722.

Holtermann, A., Gronlund, C., Karlsson, J.S., Roeleveld, K., 2008. Spatial distribution of active muscle fibre characteristics in the upper trapezius muscle and its dependency on contraction level and duration. J. Electromyogr. Kinesiol. 18 (3), 372–381.

Kelly, L.A., Kuitunen, S., Racinais, S., Cresswell, A.G., 2012. Recruitment of the plantar intrinsic foot muscles with increasing postural demand. Clin. Biomech. (Bristol, Avon) 27 (1), 46–51.

Kelly, L.A., Cresswell, A.G., Racinais, S., Whiteley, R., Lichtwark, G., 2014. Intrinsic foot muscles have the capacity to control deformation of the longitudinal arch. J. Royal Soc. Interface 11 (93).

McKeon, O.P., Hertel, J., Bramble, D., Davis, I., 2015. The foot core system: a new paradygm for understanding intrinsic foot muscle function. Br. J. Sports Med. 49 (5), 290.

Merletti, R., Parker, P., 2004. Electromyography, Physiology, Engineering and Non-invasive Applications.

Mickle, K.J., Munro, B.J., Lord, S.R., Menz, H.B., Steele, J.R., 2009. ISB Clinical Biomechanics Award 2009: toe weakness and deformity increase the risk of falls in older people. Clin. Biomech. 24 (10), 787–791.

Rathleff, M.S., Samani, A., Olesen, C.G., Kersting, U.G., Madeleine, P., 2011. Inverse relationship between the complexity of midfoot kinematics and muscle activation in patients with medial tibial stress syndrome. J. Electromyogr. Kinesiol. 21 (4), 638–644.

Richman, J.S., Moorman, J.R., 2000. Physiological time-series analysis using approximate entropy and sample entropy. Am. J. Physiol.-Heart Circulat. Physiol. 278 (6), 2039–2049.

Rodriguez-Falces, J., Negro, F., Gonzalez-Izal, M., Farina, D., 2013. Spatial distribution of surface action potentials generated by individual motor units in the human biceps brachii muscle. J. Electromyogr. Kinesiol. 23 (4), 766–777.

Rojas-Martínez, M., Mañanas, M.A., Alonso, J.F., Merletti, R., 2013. Identification of isometric contractions based on High Density EMG maps. J. Electromyogr. Kinesiol. 23 (1), 33–42.

Simon, J., Doederlein, L., McIntosh, A.S., Metaxiotis, D., Bock, H.G., Wolf, S.I., 2006. The Heidelberg foot measurement method: development, description and assessment. Gait Posture 23 (4), 411–424.

Tucker, K., Falla, D., Graven-Nielsen, T., Farina, D., 2009. Electromyographic mapping of the erector spinae muscle with varying load and during sustained contraction. J. Electromyogr. Kinesiol. 19 (3), 373–379.

Urbanek, H., Smagt, P., 2016. iEMG: imaging electromyography. J. Electromyogr. Kinesiol. 27, 1–9.

von Tscharner, V., 2000. Intensity analysis in time-frequency space of surface myoelectric signals by wavelets of specified resolution. J. Electromyogr. Kinesiol. 10 (6), 433–445.

Wakeling, J.M., Kaya, M., Temple, G.K., Johnston, I.A., Herzog, W., 2002. Determining patterns of motor recruitment during locomotion. J. Exp. Biol. 205 (3), 359–369.

Zhang, X., Zhou, P., 2012. Sample entropy analysis of surface EMG for improved muscle activity onset detection against spurious background spikes. J. Electromyogr. Kinesiol. 22 (6), 901–907.